Biochemical and Biophysical Research Communications **257,** 500–510 (1999)
Article ID bbrc.1999.0437, available online at http://www.idealibrary.com on IDEAL®

Comparison of Three Classes of Snake Neurotoxins by Homology Modeling and Computer Simulation Graphics

Hsueh-Fen Juan,* Chin-Chun Hung,† Kung-Tsung Wang,† and Shyh-Horng Chiou*,†,[1]
**Institute of Biochemical Sciences, National Taiwan University; and †Institute of Biological Chemistry, P.O. Box 23-106, Academia Sinica, Taipei, Taiwan 10098*

Received February 5, 1999

We present a systematic structure comparison of three major classes of postsynaptic snake toxins, which include short and long chain α-type neurotoxins plus one angusticeps-type toxin of black mamba snake family. Two novel α-type neurotoxins isolated from Taiwan cobra (*Naja naja atra*) possessing distinct primary sequences and different postsynaptic neurotoxicities were taken as exemplars for short and long chain neurotoxins and compared with the major lethal short-chain neurotoxin in the same venom, i.e., cobrotoxin, based on the derived three-dimensional structure of this toxin in solution by NMR spectroscopy. A structure comparison among these two α-neurotoxins and angusticeps-type toxin (denoted as FS2) was carried out by the secondary-structure prediction together with computer homology-modeling based on multiple sequence alignment of their primary sequences and established NMR structures of cobrotoxin and FS2. It is of interest to find that upon pairwise superpositions of these modeled three-dimensional polypeptide chains, distinct differences in the overall peptide flexibility and interior microenvironment between these toxins can be detected along the three constituting polypeptide loops, which may reflect some intrinsic differences in the surface hydrophobicity of several hydrophobic peptide segments present on the surface loops of these toxin molecules as revealed by hydropathy profiles. Construction of a phylogenetic tree for these structurally related and functionally distinct toxins corroborates that all long and short toxins present in diverse snake families are evolutionarily related to each other, supposedly derived from an ancestral polypeptide by gene duplication and subsequent mutational substitutions leading to divergence of multiple three-loop toxin peptides.

Snake venom toxins have become popular of late not only on the basic research fronts but also as major tools in their potential medical applications. Especially noteworthy are many reports on the characterization of varied types of small protein-type toxins from the *Elapidae* family of snakes, in particular the cobras of *Naja* genus (1–3). Among these venom components, neurotoxins, cardiotoxins and phospholipases A_2 are the three major classes of polypeptides involved in the toxicity and pharmacological actions of elapid snake bites (4).

In contrast to another prominent group of structurally similar cardiotoxins with no defined cellular targets and very diverse pharmacological functions (5), neurotoxins (α-cobratoxins) from elapid species possess well-established acetylcholine receptors and modes of action at the molecular level (6, 7). There are currently more than 100 sequences of neurotoxins determined from varied sources of snake families. It was further found that elapid neurotoxins comprised two subclasses of neurotoxins based on their molecular sizes: i.e., short chain toxins of 60–62 residues and 4 pairs of disulfide bonds versus long chain toxins of 65–74 residues and 5 pairs of disulfide bonds (2, 3). The search for the structural basis to account for different functional properties exhibited by cardiotoxins and neurotoxins has prompted us to carry out secondary and tertiary structural comparisons based on closely related primary sequences and X-ray and/or NMR structures of these toxins (8). When many homologous sequences are known for a particular class of proteins, comparative analysis of the sequence data and their corresponding tertiary structures can prove to be most informative for study of their structural relatedness.

On the basis of the previous modeling study for cobra cardiotoxins (CTXs) (8), a similar gross topology of three-loop tertiary structure is found, i.e., a core consisting of a series of short loops linked tightly by the four disulfide bridges and three flexible and protruding longer loops extending outwards. The superpositions of constructed molecular models for various CTX homo-

[1] Corresponding address: S.-H. Chiou, Institute of Biological Chemistry, Academia, P.O. Box 23-106, Taipei, Taiwan. Fax: (886)-2-3635038. E-mail: shchiou@gate.sinica.edu.TW.

0006-291X/99 $30.00

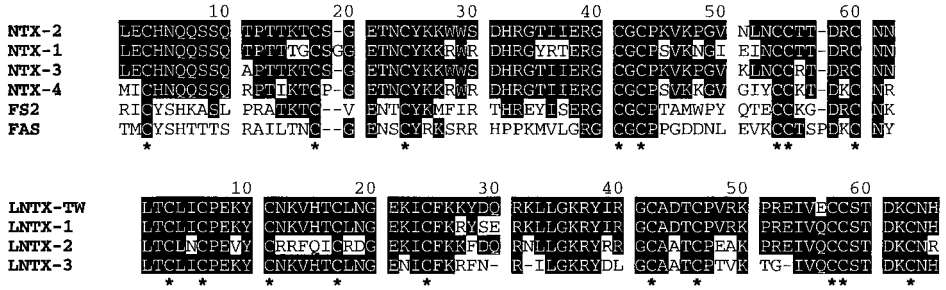

FIG. 1. Comparison of the sequences of short- and long-chain neurotoxins (NTXs) and angusticeps-type mamba toxins FS2 and fasciculin (FAS). All short and long NTX sequences listed were taken from the previous study (9 and the references therein). NTX-1 or called cobrotoxin (16) is the major short chain α-type neurotoxin from Taiwan cobra (*Naja naja atra*); NTX-2, novel NTX from Taiwan cobra; NTX-3, NTX from *Naja naja samarensis;* NTX-4, NTX from *Naja nivea;* LNTX-TW, new long chain NTX from Taiwan cobra; LNTX-1, LNTX-2 and LNTX-3 are three long chain neurotoxins from India cobra (*Naja naja naja*). The identical amino-acid residues among various sequences based on the first one (NTX-2 or LNTX-TW) are shaded in black blocks. The gaps were introduced for optimal alignment and maximum homology for the aligned sequences. The eight or ten cysteine residues situated at similar locations along the short or long chain NTXs are highlighted by asterisks. Amino acid residues are denoted by one-letter symbols.

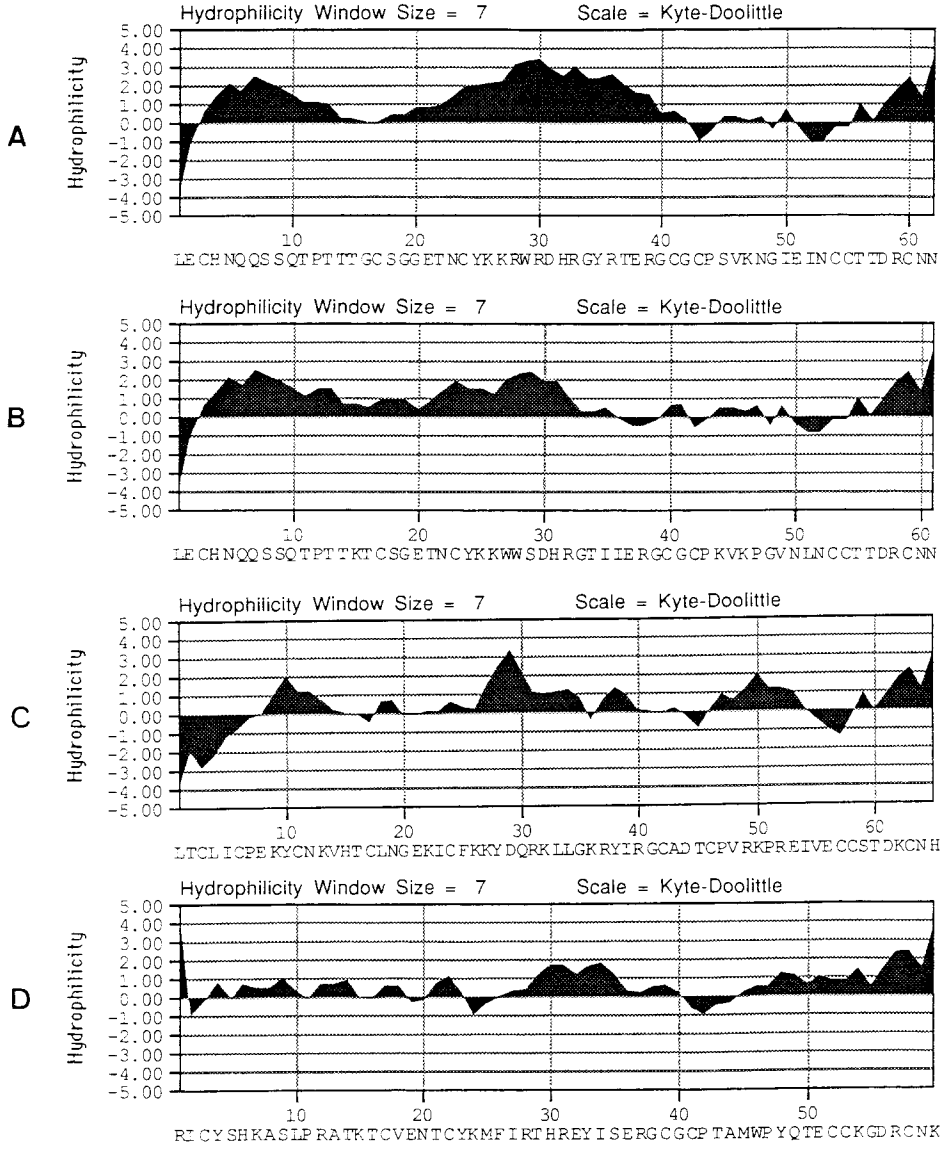

FIG. 2. Hydropathy profiles of short- and long-chain NTXs plus angusticeps-type mamba toxin FS2. The analysis of the local hydrophilicity along polypeptide sequences was based on the method of Kyte and Doolittle (14). The sequences are listed below each graph for easy comparison. It is noteworthy that NTX-1 (A) and NTX-2 (B) show similar hydropathy profiles whereas LNTX-TW (C) and FS2 (D) indicate different patterns to (A) and (B). Note that all four toxins possess mainly positive values of hydrophilicity indicative of being hydrophilic.

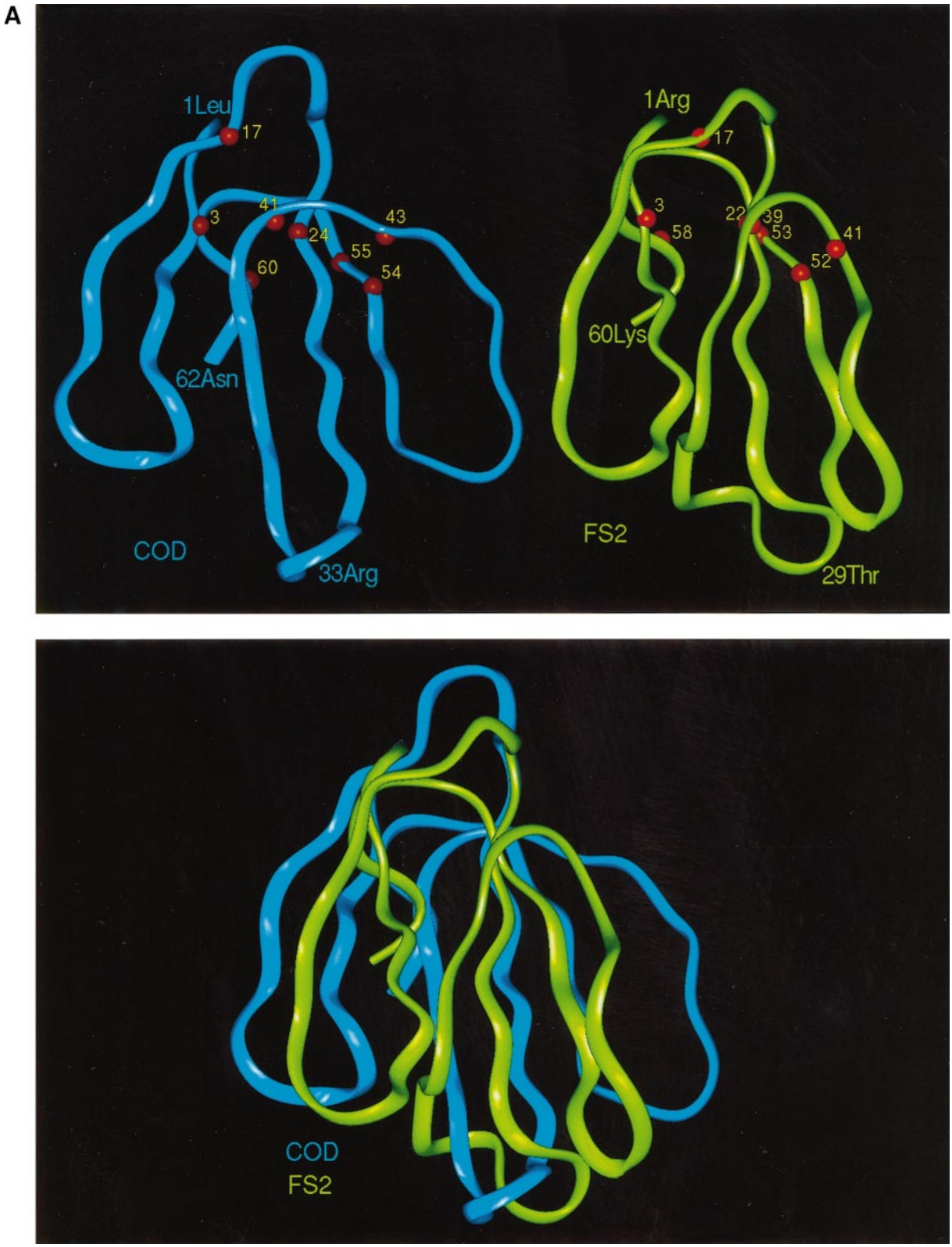

FIG. 3. Graphic ribbon models of short chain NTXs and angusticeps-type toxin FS2. Models were built based on the coordinates of NTX-1 (cobrotoxin, PDB code: 1COD) (13) and FS2 (PDB code: 1TFS) (12) derived from NMR analysis. They all show grossly similar tertiary structures with a characteristic three-loop conformation. In the model of COD, from left to right are loop I (residue #1–17), loop II (central loop, residue #23–41) and loop III (residue #42–56), respectively. The model of FS2 shows distinct folding pattern from that of COD; however, the main three-loop conformation is maintained. NTX-2 was directly modeled based on the alignment of primary sequences and COD coordinates. Superposition of the modeled structures between COD/ FS2 (**A**) and COD/ NTX-2 (**B**) is performed through the overlaying of α-carbon backbone of COD onto that of FS2 or NTX-2 while maintaining a close fit of the hydrophobic core (at the top converging end of three loops) tightly linked by disulfide bonds. In (A) the α-carbon positions for all eight cysteine residues are shown by red balls.

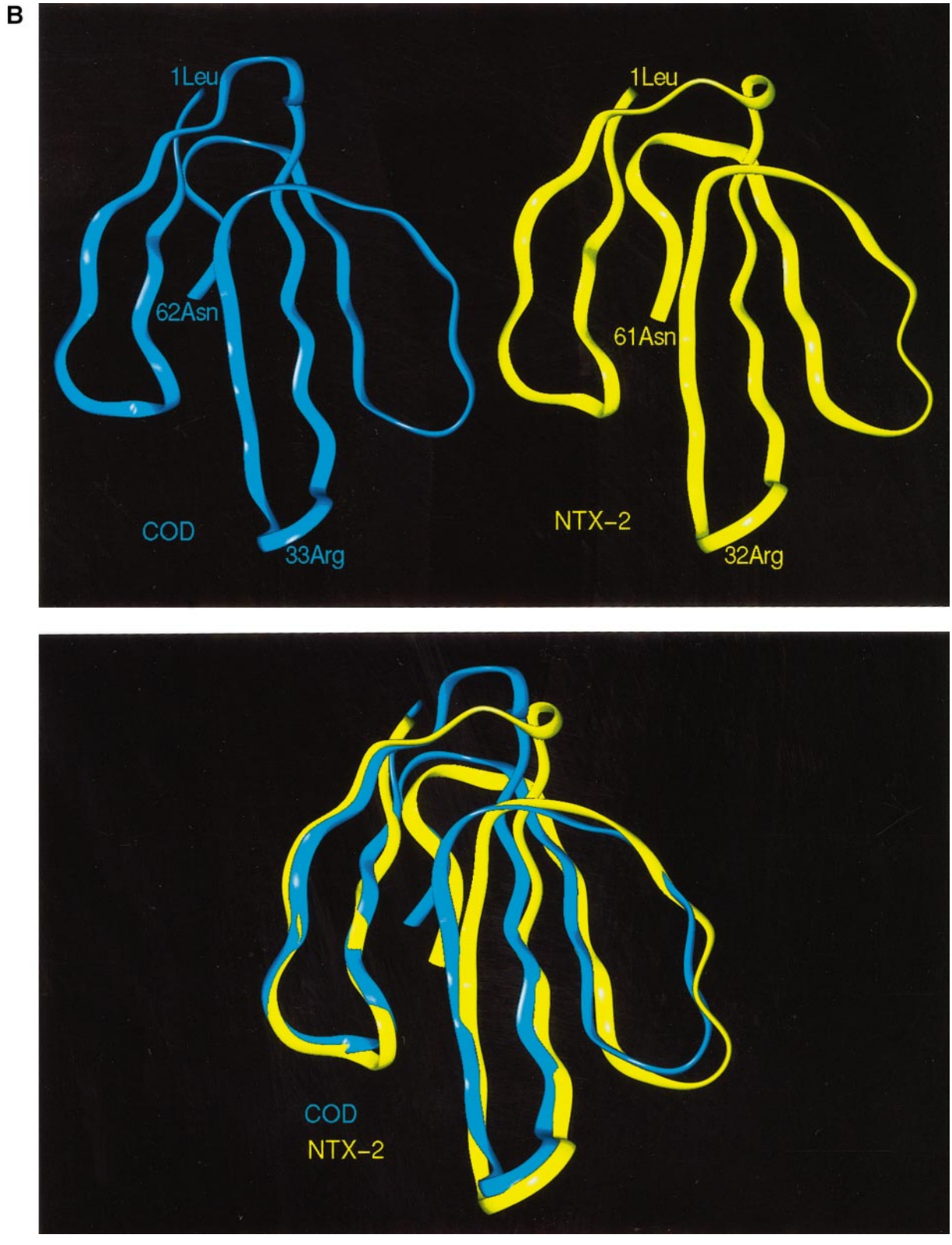

FIG. 3—*Continued*

logues indeed detected some defined and subtle structural variation along all three loops between these structurally related toxins. In this report we extend our modeling study exclusively on the other neurotoxin (NTX) family since the different functional modes of three major classes of neurotoxins may also be revealed

through their polypeptide folding patterns of respective tertiary structures simulated by homology modeling and computer graphics.

MATERIALS AND METHODS

Sample sources and sequence information of snake neurotoxins. The isolation and sequence determination of the short and long chain cobratoxins from Taiwan cobra were as described in the previous report (9). The sequence of the angusticeps-type toxin (denoted as FS2), a major component of the black mamba snake family, was taken and cited from previous reports (10, 11). The NMR structures of FS2 (12) and the short chain α-type cobrotoxin (13) were used as the structural basis for homology modeling of two newly discovered short and long chain neurotoxins reported recently from our group (9).

Secondary structure prediction and hydrophobicity profile. Secondary structure prediction using the Mac Vector sequence analysis algorithm softwares (International Biotechnologies, Inc., New Haven, CT) was carried out on the Macintosh computer as described previously (8). The surface hydrophobicity profile based on the empirical Kyte-Doolittle hydropathy scale (14) of peptide segments in a protein was plotted along each toxin sequence. For graphing purpose the signs of the hydropathy values have been reversed in order to plot the hydrophilicity instead of hydrophobicity scale. A window of size N=7 is run along the length of the protein; for each window, the hydropathy values of 7 amino acids are summed and divided by 7 to obtain the average hydrophilicity per residue for the window. Values above the axis denote hydrophilic regions which may be exposed on the outside of the analyzed molecule whereas those values below the axis indicate hydrophobic regions which tend to be buried inside the toxin molecule.

Homology modeling and computer graphics of structurally related toxins. The sequences of the short and long chains of cobratoxins (9) and the angusticeps-type toxin (denoted as FS2) were aligned concurrently to locate sequence-conserved regions. The coordinates of one short chain neurotoxin derived from NMR analysis (13), i.e., cobrotoxin from Taiwan cobra, were used as a template for model building of two newly-discovered cobratoxins by employing the graphics program Insight II (Biosym, 1995) on a Silicon Graphics INDY workstation. Under Homology Module of Insight II environment, multiple sequence alignment algorithm was used to align the short and long chains of cobratoxin sequences to the sequence of cobrotoxin isolated from the same Taiwan cobra venom. The main-chain coordinates of modeled short and long chain cobratoxins were simulated from the existing cobrotoxin structure derived from NMR spectroscopy (13) and compared with that of the NMR-derived FS2 toxin structure (12). The coordinates of the side-chain and undefined terminal residues were assembled and relaxed by using "End Repair" and "Relax" functions in Homology Module, which both use the "Discover" program with "CVFF" forcefield to remove close contacts and reduce structural strains. The complete structures were further minimized by heating up to 300 °K, equilibration for 0.5 ps (500 steps), 200 steps of steepest gradient minimization and 10,000 steps of conjugate gradient minimization to optimize the hydrogen bonds, ion pairs and hydrophobic interactions. For pair-wise comparisons of modeled short and long chain neurotoxin structures with the solution structure of cobrotoxin determined from NMR, we first input the sequences of these two NTXs into the multiple sequence alignment algorithm to obtain two modeled short chain (NTX-2) and long chain (LNTX-TW) structures simulated and derived from the NMR coordinates of cobrotoxin (1COD). In general the average RMS (root-mean-square) deviations for most of the backbone atoms of these toxin molecules are estimated in order to assess the validity and relative accuracy of homology modeling and computer simulation graphics.

Construction of a phylogenetic tree for postsynaptic neurotoxins. A software package of LaserGene of Macintosh version (DNASTAR Inc., Madison, WI) was used for the estimation of sequence homology based on percent similarity and divergence among different toxin sequences. Percent divergence is estimated by comparing sequence pairs based on phylogenetic relationships. In contrast the percent similarity is obtained by comparing sequences directly without considering phylogenetic relationships. The phylogenetic or evolutionary tree was then constructed using the algorithm of Hein (15) in the MegAlign programs of the LaserGene package. It is a multiple-sequence alignment program that builds trees as it aligns protein sequences using a combination of distance matrix and approximate parsimony methods. This phylogeny analysis program makes multiple alignments by imposing restrictions based on evolutionary relatedness of various aligned sequences, which is useful to align highly evolved gene families that have clear evolutionary relationships such as multiple snake neurotoxin isoforms reported here.

RESULTS AND DISCUSSION

Understanding the complex evolutionary mechanism for the generation of structurally related proteins from phylogenetically close or remote species remains a general biological problem. Especially noteworthy is the abundant distribution of multiple snake toxin molecules in the *Elapidae* and *Hydrophidae* families which include most terrestrial cobras and sea snakes respectively. There are currently more than 100 small postsynaptic neurotoxins with high sequence homology being isolated and characterized, in particular those short neurotoxins (60–62 amino acids and 4 disulfide bridges), and long neurotoxins (65–74 amino acids and 5 disulfide bridges) from the Naja genus of elapid snakes (2). The venom of Taiwan cobra (*Naja naja atra*) is extremely lethal when compared with those of crotalid and viperid snakes. One short neurotoxin (named cobrotoxin) (16) consisting of 62 amino-acid residues has previously been characterized as the major principal neurotoxic component from this cobra. In the present study we compare two novel neurotoxin isoforms isolated from the same crude venom of Taiwan cobra (9) with cobrotoxin and another angusticeps-type toxin (denoted as FS2) from the black mamba snake family of Africa. In order to gain some insight into the structure-function correlation of three classes of neurotoxins with some sequence homology, it is deemed essential to compare these toxins based on X-ray and/or NMR data coupled with state-of-the-art computer-graphic simulation modeling in order to reveal minor structural differences among these analogous toxins, which may account for their functional diversity at the molecular level.

Multiple sequence alignment of venom toxins. Figure 1 shows multiple sequence alignments for the comparative analysis of various short and long chain NTXs plus toxin FS2 of black mamba, a specific blocker of the L-type calcium channel. It was found that short chain NTXs (NTX-1 to NTX-4) of different elapid snakes show about 74–95% sequence similarity whereas the sequence homology for long chain NTXs (LNTX-1 to LNTX-3 plus LNTX-TW) is found to be about 67–94%. It is noteworthy that short- and long-chain NTXs show

TABLE 1

Hydrophobicities, Isoelectric Points and Molecular Weights of Various Neurotoxin Homologues

	NTX-2	NTX-1	NTX-3	NTX-4	FS2	FAS	LNTX-TW	LNTX-1	LNTX-2	LNTX-3
Hϕ	−0.95	−1.20	−0.98	−0.98	−0.73	−0.78	−0.56	−0.54	−0.60	−0.19
pI	8.07	8.07	8.49	9.45	8.64	8.26	8.61	8.8	8.82	8.28
Mr	6833	6956	6873	6975	7027	6757	7568	7568	7637	6943

Note. Hϕ is the hydrophobicity index as defined by Kyte and Doolittle (1982). pI and Mr denote isoelectric points and molecular weights calculated from the primary sequences of various neurotoxin homologues.

only 28–33% sequence identity, corroborating the remote relationship between the two classes. In general due to the presence of one extra pair of disulfide bond in long-chain NTX it is more difficult to have an optimal alignment between these two classes of NTXs for homology comparison. This certainly underlines the unusual evolutionary relationship between these two classes of NTXs and deserves a further study on their tertiary structures by homology modeling (see below).

In Fig. 1 we have also included FS2 and fasciculin (FAS) for comparison, both being members of angusticeps-type toxins from the mamba snake family and showing a similar molecular size to short chain NTXs and no neurotoxic activity. With proper arrangement of 8 or 10 structurally conserved cysteine residues at their relatively identical positions, the optimal alignment can be made by introducing a minimum number of gaps along the entire lengths of these short and long chain toxin sequences. Without exception short- and long-chain NTXs separately shows good matches in amino acid identity along their polypeptide chains whereas high variation in protein sequences is detected between short- and long-chain NTXs or short chain NTXs and FS2/FAS. However sequence variation in each class of NTXs seem to be fairly conservative, indicating a preservation of a common structure in each class of NTXs.

Surface hydrophobicity and hydropathy profiles of elapid toxins. We have compared the general distribution of surface-charge groups in these structurally related toxins by using the analysis program of surface hydrophilicity in these sequences based on the Kyte-Doolittle hydropathy scale (Fig. 2). Cobrotoxin (NTX-1) (Fig. 2A) and our newly characterized short chain cobratoxin (NTX-2) (Fig. 2B) show similar hydropathy patterns, which are different from those of long-chain neurotoxin (LNTX-TW) (Fig. 2C) and angusticeps-type toxin FS2 (Fig. 2D). All these elapid toxins show prominent positive hydrophilicity along the sequences, indicative of their polypeptide chains being probably easily exposed to solvent and very soluble in aqueous solution. It is also of interest to note that all these elapid NTXs are almost devoid of α-helical structures when analyzed by a secondary-structure prediction algorithm of Mac Vector sequence analysis software (data not shown). The dominance of β-sheet and β-turns secondary structure in these toxins is in general consistent with CD and Raman studies of these toxins (17, 18). Table 1 shows hydrophobicity indices Hϕ for all toxin sequences calculated by using the hydrophobic scale of Kyte-Doolittle (14) together with their respective isoelectric points (pI) and molecular weights (Mr) for comparison. The negative hydrophobicity indices (Hϕ) which were calculated for all neurotoxins is in accord with the hydropathy profiles shown for the four representative toxins in Fig. 2. Therefore it points to the fact that neurotoxins of these three major classes are mainly hydrophilic short polypeptides with basic pIs. These determined sequences should provide a solid basis not only for a preliminary secondary-structure prediction but also basic information for the construction of tertiary structures based on the coordinates obtained from the X-ray and/or NMR structural analysis of homologous toxins.

Homology modeling and computer graphics of neurotoxins. Homology model-building based on the primary sequences and the established NMR structures of homologous toxins has revealed a grossly similar structure shared by three classes of snake toxins, i.e., a three-loop tertiary structure with eight or ten critically important cysteines situated at the base to form a hydrophobic core and three flexible external loops extending outwards.

Figure 3A illustrates the folding and arrangement of polypeptide chains adopted as the basis reference protein sets for modeling, i.e., a short chain neurotoxin NTX-1 (cobrotoxin, PDB code: 1COD) (13) and an angusticeps-type toxin FS2 (PDB code: 1TFS) (12). The gross topology of these basis polypeptides is somewhat similar, a tertiary structure with three-fingered loops extending from a more compact core held tightly by 4 pairs of disulfide bonds at the top of the toxin molecules. The amino acid sequence of NTX-1 from Taiwan cobra, which was used as the basis reference for modeling is similar to our newly characterized short chain NTX-2 (sequence identity is about 80.3%). Therefore it is to be expected that the tertiary structures of these two short chain NTXs would certainly be similar regarding their solution structures. On the other hand, NTX-1 and FS2 share only 42.6% sequence similarity

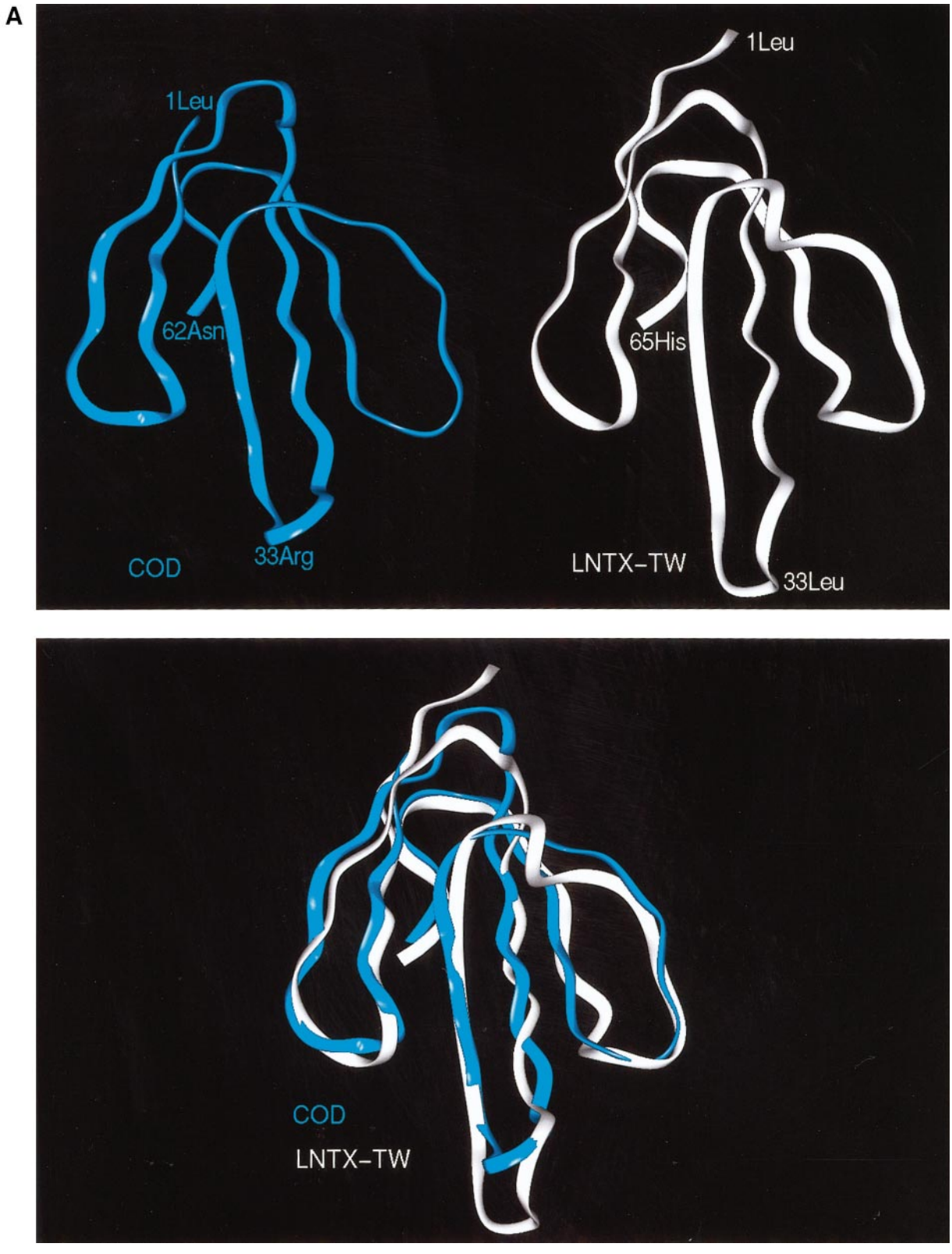

FIG. 4. Graphic ribbon models of long chain NTXs and stereoviews at the tip ends of loop I and loop II. Long neurotoxin of Taiwan cobra (LNTX-TW) was built based on the coordinates of NTX-1 (cobrotoxin, PDB code: 1COD) (13) derived from NMR analysis. It shows a similar tertiary structure to short chain NTX-2 (Fig. 3B) with a characteristic three-loop conformation. Superposition of the modeled structures between COD and LNTX-TW (**A**) is performed through the overlaying of α-carbon backbone of COD onto that of LNTX-TW while maintaining a close fit of the hydrophobic core tightly linked by disulfide bonds. In (**B**) the stereoviews of the tip regions of loop I (residues #6–11 of NTX-2 and residues #9–14 of LNTX-TW) and loop II (residues #29–34 of NTX-2 and residues #30–34 of LNTX-TW) are shown for three neurotoxins in stick models to highlight the similarity of relative orientation and conformational turn at the tip regions of these loops between short chain NTXs and some distinct differences between short and long chain NTXs.

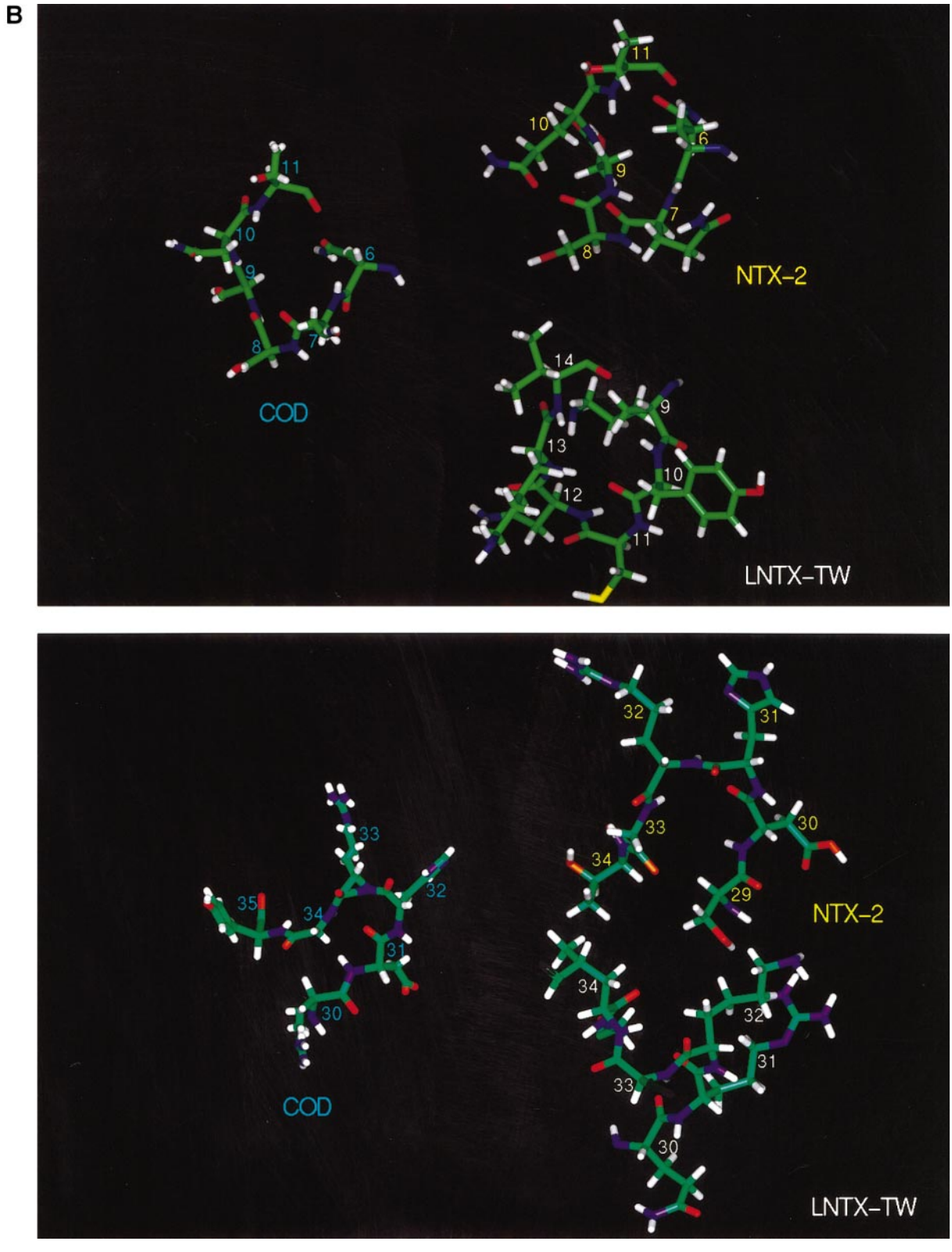

FIG. 4—*Continued*

which might be too low for a meaningful homology modeling. Therefore the modeled structure of FS2 was directly taken from the derived NMR structure of this toxin (Fig. 3A), which is expected to show some detailed differences in backbone folding from that of COD structure.

TABLE 2

Comparison of RMSD (Root-Mean-Squared Deviation) among Three Loops

	COD	NTX-2	RMSD*
Loop I	Residue 6–11	Residue 6–11	0.799392
Loop II	Residue 30–35	Residue 29–34	0.953584
Loop III	Residue 47–51	Residue 46–50	0.630174
	COD	LNTX-TW	RMSD
Loop I	Residue 6–11	Residue 6–11	0.893123
Loop II	Residue 30–35	Residue 30–35	1.902800
Loop III	Residue 47–51	Residue 49–53	0.769580

* All RMSD are expressed in Å.

It is well known that the definite structures of peptide loops with some degrees of flexibility are usually very difficult to be calculated precisely from NOE restraints of NMR spectroscopy measured for proteins in solution. Upon superposition of 1COD with NTX-2 (Fig. 3B) it is clearly indicated that the fitting between the two is generally very good except one linking short loop at the core region and small unfitted and flexible short coil at the tip region of loop III. Careful scrutiny of these superimposed models of COD/NTX-2 (Fig. 3B) and COD/LNTX-TW (Fig. 4A) indicated that the major conformational difference between the homologues of short chain NTXs is quite small and that between short and long chain NTX only lies in the far end region (residues #30–34 in LNTX-TW) of loop II with loops I and III superimposed nicely on each other.

We have listed and compared RMS deviation or difference (RMSD) in Table 2 to assess the fitness and relative accuracy of structural superposition for the corresponding end regions of three flexible loops in short and long chain NTXs. It is shown that the fitting of modeled structures between short chain NTXs (COD/NTX-2) is much better than that between short and long chain NTXs (COD/LNTX-TW) with a significantly lower RMSD values in the former than the latter. The conformation of loop II is different from loop I and III, and the RMS deviation after superposition is larger and more variable based on the coordinates of the derived NMR structure of 1COD (13). The higher values obtained for RMSD in the tip region of loop II for COD/NTX-2 and COD/LNTX-TW than those in loops I and III is indicative of the higher flexibility in this target region of the central loop, which has also been proposed as the specific domain for their interaction with the nicotinic acetylcholine receptor (19, 20). Major differences have also been observed in the conformation of the central loop (loop II, residues #23–42, COD numbering) between COD and FS2, resulting in a change of orientation in the concavity of these two classes of toxin molecules (12, 21, 22). The overall concavity of the FS2 molecule, considered as a flat bottomed dish, is oriented toward the C-terminal loop (loop I) of the molecule whereas that of short and long chain NTXs is oriented towards opposite direction. Loop I of FS2 appears to be less well defined and more flexible than the same loop for NTXs. The described differences could be some of the factors leading to distinct pharmacological properties for angusticeps-type toxins and cobra NTXs.

Generally speaking, these two modeled NTXs possess average RMS deviations of less than 1.0 Å for their backbone atoms relative to the average structure derived from NMR analysis of short chain NTX-1 with the exception of long chain NTX extending a longer loop over the end region of loop II than short chain NTX, which results in a much higher RMSD of 1.90 Å (Table 2 and Fig. 4A) for loop II modeling in LNTX-TW. In Fig. 4B we show the stereo diagrams of peptide segments in the end region of loop I (residues #6–11 and #9–14) and loop II (residues #29–34 and #30–34) for short and long chain NTXs as compared with the reference toxin COD structure. The orientation and peptide bending patterns of these four short loops appear to differ considerably, which are the consequences of variations in their amino acid sequences and might be involved in the correct positioning and alignment of functionally important residues in these loop segments (12, 21).

Construction of a phylogenetic tree among three classes of elapid toxins. In our systematic pair-wise sequence comparison of crystallin genes and their deduced protein sequences from varied species of animal kingdom, a higher sequence homology is generally found between cDNA sequences than protein sequences (23–25). However it appears to be more sensitive to detect sequence divergence based on protein sequences than cDNA sequences when comparing highly homologous protein families. In Fig. 5 a phylogenetic tree is constructed based on some short- and long-chain toxin sequences comprising representative members of three major classes of elapid toxins using the algorithm of Hein (15), which is a multiple sequence alignment program that builds trees as it aligns phylogenetically related protein sequences using a combination of distance matrix and approximate parsimony methods. The results indicate that the phylogenetic tree based on the sequence divergence among these toxin sequences indeed exemplifies the close relatedness between various toxin members of short-chain or long-chain NTX class. It is noteworthy that three major classes of elapid toxins are all found to locate at different branching points of the phylogenetic tree, with the class of angusticeps-type toxins (FS2 and fasciculin) being placed closer to short chain than long chain NTXs. Based on the derived phylogenetic rela-

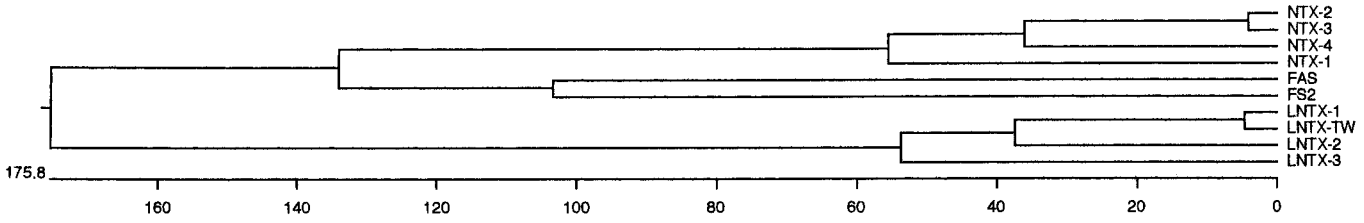

FIG. 5. Construction of a phylogenetic tree of short- and long-chain neurotoxins (NTXs) plus angusticeps-type mamba toxins FS2 and fasciculin (FAS). A phylogenetic analysis software of Hein (15) was used to construct a tree based on the percent divergence between protein sequences using a combination of distance matrix and approximate parsimony methods. Percent divergence is calculated by comparing sequence pairs in relation to the relative positions in the phylogenetic tree. This algorithm carries out multiple-alignment by imposing restrictions based on evolutionary relatedness of the aligned sequences. The length for each pair of branches represents the sequence divergent distance between aligned pairs. The scale beneath the tree measures the distance between sequences (in millions of years).

tionships, the divergence of short chain NTX and angusticeps-type mamba toxins appears to occur much later than that of short and long chain NTXs. It also leads to the supposition that short- and long-chain NTXs diverged from the common ancestral neurotoxin molecule and the evolutionary rate (percent sequence divergence) for short-chain NTX and FS2 is much higher than long-chain NTX.

CONCLUSION AND PERSPECTIVES

The search for a structural or molecular basis to account for the different pharmacological actions of cardiotoxins and neurotoxins from cobra venom has prompted us to characterize various toxins such as cardiotoxins (8) and neurotoxins (this report) by homology modeling and computer simulation graphics. These two functionally distinct classes of snake toxins share a common tertiary structure as determined by X-ray and/or NMR analysis, a core consisting of a series of short loops and four disulfide bridges plus three finger-like flexible loops. Multiple sequence alignment and comparison coupled with homology modeling and computer simulation for two newly discovered short and long chain NTXs from Taiwan cobra have essentially corroborated similar structural features reported for homologous toxins from different species.

The results suggest that such a homology modeling/computer graphics approach in the absence of X-ray or NMR data could provide some insight into the molecular interaction between peptide toxins and their intended biological targets. There is much additional insights to be gained by the detailed structural comparison of these sequence-related toxin analogues in order to provide a means of correlating structure/function properties. It is established that all nicotinic α-neurotoxins present in the snake family of *Elapidae* are closely related to each other in terms of primary and tertiary structures, presumably these snake toxins being derived from an ancestral polypeptide by gene duplication and subsequent multiple mutational substitutions.

ACKNOWLEDGMENTS

This work was supported in part by Academia and the National Science Council (NSC Grants 87-2311-B-002-068 and 88-2311-B-002-061 to S.-H. Chiou), Taipei, Taiwan. This report will be submitted as part of a dissertation by H.-F. Juan to National Taiwan University in partial fulfillment of the degree of Doctor of Philosophy.

REFERENCES

1. Lee, C. Y. (1979) *in* Advances in Cytopharmacology (Ceccarelli, B., and Clementi, F., Eds.), Vol. 3, pp. 1–16, Raven Press, New York.
2. Karlsson, E. (1979) *in* Snake Venoms, Handbook of Experimental Pharmacology (Lee, C. Y., Ed.), Vol. 52, pp. 159–212, Springer, Berlin.
3. Dufton, M. J., and Hider, R. C. (1983) *CRC Critical Rev. Biochem.* **14,** 113–171.
4. Dufton, M. J., and Hider, R. C. (1988) *Pharmac. Ther.* **36,** 1–40.
5. Lee, C. Y., Chang, C. C., Chiu, T. H., Chiu, P. J. S., Tseng, T. C., and Lee, S. Y. (1968) *Naunyn-Schmiedebergs Arch. Pharmak.* **259,** 360–374.
6. Changeux, J. P. (1981) *Harvey Lect.* **75,** 85–254.
7. Ruan, K.-H., Spurlino, J., Quiocho, F. A., and Atassi, M. Z. (1990) *Proc. Natl. Acad. Sci. USA* **87,** 6156–6160.
8. Chiou, S.-H., Hung, C.-C., Huang, H.-C., Chen, S.-T., Wang, K.-T., and Yang, C.-C. (1995) *Biochem. Biophys. Res. Commun.* **206,** 22–32.
9. Hung, C.-C., Wu, S.-H., and Chiou, S.-H. (1998) *J. Protein Chem.* **17,** 107–114.
10. Strydom, D. J. (1976) *Eur. J. Biochem.* **69,** 169–176.
11. Strydom, D. J. (1977) *Eur. J. Biochem.* **76,** 99–106.
12. Albrand, J.-P., Blackledge, M. J., Pascaud, F., Hollecker, M., and Marion, D. (1995) *Biochemistry* **34,** 5923–5937.
13. Yu, C., Bhaskaran, R., Chuang, L.-C., and Yang, C.-C. (1993) *Biochemistry* **32,** 2131–2136.
14. Kyte, J., and Doolittle, R. F. (1982) *J. Mol. Biol.* **157,** 105–132.
15. Hein, J. (1990) *Methods Enzymol.* **183,** 626–645.
16. Yang, C. C. (1965) *J. Biol. Chem.* **240,** 1616–1618.

17. Grognet, J.-M., Menez, A., Drake, A., Hayashi, K., Morrison, I. E. G., and Hider, R. C. (1988) *Eur. J. Biochem.* **172,** 383–388.
18. Chiou, S.-H., Lee, B.-S., and Yu, N.-T. (1992) *Biochem. International* **26,** 747–758.
19. Pillet, L., Tremeau, O., Ducancel, F., Drevet, P., Zinn-Justin, S., Pinkasfeld, S., Boulain, J.-C., and Menez, A. (1993) *J. Biol. Chem.* **268,** 909–916.
20. Fiordalisi, J. J., Al-Rabiee, R., Chiappinelli, V. A., and Grant, G. A. (1994) *Biochemistry* **33,** 12962–12967.
21. Brown, L. R., and Wüthrich, K. (1992) *J. Mol. Biol.* **227,** 1118–1135.
22. Hatanaka, H., Oka, M., Kohda, D., Tate, S., Suda, A., Tamiya, N., and Inagaki, F. (1994) *J. Mol. Biol.* **240,** 155–166.
23. Chiou, S.-H., Yu, C.-W., Lin, C.-W., Pan, F.-M., Lu, S.-F., Lee, H.-J., and Chang, G.-G. (1995) *Biochem. J.* **309,** 793–800.
24. Lu, S.-F., Pan, F.-M., and Chiou, S.-H. (1995) *Biochem. Biophys. Res. Commun.* **216,** 881–891.
25. Pan, F.-M., Chang, W.-C., Lu, S.-F., Hsu, A.-L., and Chiou, S.-H. (1995) *Biochem. Biophys. Res. Commun.* **217,** 940–949.